Unraveling the reactivity of minium towards bicarbonate and the role of lead oxides therein

Unraveling the reactivity of minium towards bicarbonate and the role of lead oxides therein

Eyasu Ayalew, Koen Janssens and Karolien De Wael*

AXES Research Group, Department of Chemistry, University of Antwerp, Groenenborgerlaan 171, B-2020 Antwerp, Belgium

*Author to whom correspondence should be addressed. Tel: 0032-3-265-33-35; e-mail: Karolien.DeWael@uantwerpen.be

ABSTRACT: Understanding the reactivity of (semiconductor) pigments provides vital information on how to improve conservation strategies for works of art in order to avoid rapid degradation of the pigments. This study focuses on the photoactivity of minium (Pb_3O_4), a semiconductor pigment, that gives rise to strong discoloration phenomena upon exposure to various environmental conditions. To demonstrate its photoactivity, an electrochemical setup with minium-modified graphite electrode ($C|Pb_3O_4$) was used. It is confirmed that minium is a p-type semiconductor which is photoactive during illumination and becomes inactive in the dark. Raman measurements confirm the formation of the degradation products. The photoactivity of a semiconductor pigment is partly defined by the presence of lead oxide (PbO) impurities; these introduce new states in the original band gap. It will be experimentally evidenced that the presence of PbO particles in minium leads to an upward shift of the valence band that reduces the band gap. Thus, upon photoexcitation, the electron/hole separation is more easily initialized. The PbO/Pb_3O_4 composite electrodes demonstrate a higher reductive photocurrent compared to the photocurrent registered at pure PbO or Pb_3O_4 modified electrodes. Upon exposure to light with energy close to and above the band gap, electrons are excited from the valence band to the conduction band to initialize the reduction of Pb(IV) to Pb(II), resulting in the initial formation of PbO. However in the presence of bicarbonate ions, a significantly higher photoreduction current is recorded since the PbO reacts further to form hydrocerussite. Therefore the presence of bicarbonates in the environment stimulates the photodecomposition process of minium and plays an important role in the degradation process.

KEYWORDS: MINIUM; PIGMENT; SEMICONDUCTOR; DEGRADATION; ELECTROCHEMISTRY; RAMAN

1. INTRODUCTION

The mineral minium, also known as red lead, is a brilliant orange-red mixed valence compound containing lead atoms both in the Pb(II) and Pb(IV) states. Depending on the presence of impurities in this material, there may be slight differences in colour.[1] It was one of the earliest pigments prepared artificially and has been widely used for the decoration of wall and panel paintings as well as manuscripts of the medieval period.[2, 3] However, its application as an artistic pigment or as an ingredient in anticorrosive paint on iron and steel has steadily declined due to its toxicity. Nowadays its application is mainly as an electrode material in batteries[4, 5] and as an additive in the manufacture of glass.[6]

In this article, we will focus on the semiconducting properties of minium as these properties give rise to strong discoloration phenomena of the material. Semiconductors are characterized by a fully occupied valence band (VB) and an unoccupied conduction band (CB) separated by E_g (energy gap), usually below 4 eV. During exposure to light of appropriate energy (wavelength), electrons are excited from the valence band to the conduction band inducing conductivity. The photoactivity depends on the energy of the incoming light and the band gap energy of the semiconductor. The latter is ~2.1 eV in the case of minium.[7] The top of the valence band of Pb_3O_4 consists mainly of Pb(II)(6s) states while the bottom of the conduction band is dominated by Pb(IV)(6s) states. Depending on accumulation of holes or electrons in the crystal structure of the compound, semiconductors could be either p-type or n-type. Minium is a p-type semiconductor characterized by accumulation of negative surface charge. The holes are the majority carriers and the Fermi level is found closer to the valence band. Upon exposure to light, electrons are excited to the conduction band where they are taken up by the Pb(IV) ions and hence reduction reactions are expected to take place, initiating the degradation of the pigment.

Environmental conditions such as temperature, light, relative humidity and the presence of other chemicals in the surrounding medium significantly affect the behavior of semiconductor pigments. In minium-paint degradation studies, blackening and whitening (depending on specific environmental conditions) are the two most commonly described phenomena. Minium darkening is mainly due to the formation of lead sulphide (PbS) and/or lead dioxide (PbO_2). In the case of whitening either lead carbonates such as $PbCO_3$ and $Pb_3(CO_3)_2(OH)_2$ or lead sulphate ($PbSO_4$) are identified as degradation products.[8-12] It is also reported that the presence of CO_2 in the environment is a key factor in the photodegradation process of minium. The CO_2 can be either introduced into the porous paint layers from the atmosphere[13] or may be locally formed from the oxidative decarboxylation of the binding medium.[14] Recently x-ray powder diffraction techniques were used to investigate minium degradation products from real paint samples and plumbonacrite ($3PbCO_3.Pb(OH)_2.PbO$), was found to be present.[15] In this article, an experimental design was followed to clarify the role of carbonates/bicarbonates in the photodegradation process of minium.

Additionally, the role of lead oxide impurities, present in the minium because of incomplete synthesis, on the photoreactivity of the pigment is investigated. It has been documented that real samples of minium contain variable amounts of impurities usually in the form of lead (II) oxide (PbO).[16, 17] PbO occurs in tetragonal and orthorhombic structural forms as litharge (α-PbO) and massicot (β-PbO) respectively. These two compounds also exhibit semiconducting behavior with characteristic absorption edges (Figure 1). The presence of such impurities plays a significant role in modifying the reactivity (photoactivity) of semiconductor materials. Therefore, litharge (α-PbO), which remains behind as an impurity during minium synthesis[18], could influence the photoactivity of the pigment. In this study both pure minium (commercial, analytical grade) and synthesized minium containing ca. 5 % of α-PbO (determined by XRD) were used to explore the role of PbO.

Lately electrochemistry is being used as a fast technique for identifying pigment degradation products and as a tool for monitoring pigment degradation processes in the aim of predicting harmful/favorable environmental conditions.[19] This method does not require lengthy exposure of the pigments to (chemical or physical) degrading agents in an artificial ageing chamber. Therefore, the electrochemical set up was used to investigate the influence of light on the reactivity of minium by varying the type of

electrolytes and by doping the pigment with impurities such as lead oxides in order to mimic the composition of realistic minium samples in a humid environment. A deeper understanding into the electronic structure of the pigment and the role of lead oxide impurities is crucial in defining its photoreactivity having an immense importance towards the ongoing efforts of conserving valuable works of art.

2. EXPERIMENTAL

Sample preparation

Two types of minium (Pb_3O_4) were used in this study: on the one hand, pure minium was commercially obtained (Alfa Aesar company, 97 % purity with 3 % total metal impurities) while it was also self-synthesized. The synthesized minium was prepared by calcination of lead nitrate at 753K for 30 hours in a limited amount of flowing oxygen as discussed in[16, 20]; the material obtained in this manner contains ca. 5 % litharge (α-PbO). In the text, we refer to this compound as 'synthesized minium'. Before immobilization on the electrode surface, the powder was first ground with a mortar to allow a better contact with the surface of the electrode. In the interest of obtaining a rough surface, the graphite working electrodes were pretreated by polishing with a P400 SiC paper. The ground powder (0.05 g) was suspended in 1 mL of absolute ethanol and 1 μL of the minium-ethanol suspension was pipetted out to modify the surface of the graphite electrodes. The surface of the pigment modified electrode was allowed to dry before the electrochemical measurements.

In order to understand the role of lead oxides in the photoactivity of minium, pure litharge was synthesized from lead acetate while commercial massicot (ACS reagent ≥ 99.0 %) was purchased from Sigma-Aldrich. The procedure for preparation of pure litharge is discussed in Ref. [21]. In a similar way, the α-PbO and β-PbO semiconductor nanoparticles were ground into a fine powder, suspended in absolute ethanol before immobilization on the surface of the electrode for electrochemical study. Chemicals used in this study i.e. sodium carbonate, sodium bicarbonate and sodium chloride were purchased from MERCK (Germany) and were of analytical grade.

Electrochemical measurements

Electrochemistry is a useful analytical technique in the identification of heritage materials such as pigments and dyes. The oxidation state of electroactive species in the sample enables an easy discrimination and due to the high sensitivity of the electrochemical methods, only small amount of sample material (nanograms) is necessary. In this study, a three electrode electrochemical set up[19] is used with a graphite working electrode containing the sample under investigation, a reference electrode (Ag|AgCl) setting the potential of the solution and a counter electrode (Pt) completing the electronic circuit. Minium-modified graphite electrode ($C|Pb_3O_4$) was used to study the semiconductor behavior and to demonstrate the photoactivity of the pigment. Both 0.01 M NaCl (pH=7) and $Na_2CO_3/NaHCO_3$ (pH=8-11) electrolytes were used in the experiments involving alternating cycles of darkness (~ 10 s) and illumination (~ 10 s) from a blue laser (405 nm, 30 mW). Red Laser (650 nm, 30 mW) was also used to test the photoreactivity of the pigment at energy below its band gap. All electrochemical experiments were performed using a μ-Autolab potentiostat or Galvanostat PGSTAT from Metrohm (The Netherlands), controlled by NOVA 1.10 software.

Analytical characterization

Absorption spectra of Pb_3O_4, α-PbO, β-PbO and synthesized minium were characterized via diffuse reflectance UV-vis spectrophotometry to define the band gap energy of the products. The pigment powders (0.02 g) were blended and crushed with KBr (0.985 g) dried at 200°C. The spectra were recorded using a Thermo Electron Nicolet Evolution 500 UV-VIS spectrophotometer equipped with an RSA-UC-40 diffuse reflectance accessory in the wavelength range of 250–850 nm.

Raman spectra were collected with an inVia spectrometer (Renishaw PTY Ltd.) utilizing the 514.5 nm (green) and 785 nm (red) excitation lines with maximum power of 50 mW (20 mW delivered at the sample). The grating was calibrated using the 520 cm^{-1} silicon band. Exposure time, number of acquisitions and laser power varied from 1 to 10 s, 1 to 100 and 2 to 10 mW, respectively. Spectral manipulations such as baseline adjustment, smoothing and normalization were performed with the Renishaw WiRE 2.0 software.

3. RESULTS AND DISCUSSION

3.1 UV-Vis-DR to define and compare the band gaps

The acquired UV-Vis-DR (UV-Visible Diffuse Reflectance) spectra clearly reflect the semi-conducting behavior of the materials with distinct absorption edges (Figure 1). The onset wavelength for each semiconductor material was determined by drawing a tangent line over the most vertical area of the spectra. A conversion factor (equation 1) between wavelength and band gap from the energy of photon formula was applied to calculate the band gap of the materials. The band gap energies for commercial (orange curve) and synthesized minium (green curve) is calculated to be 2.05 and 1.98 eV respectively.

$$\lambda(nm) \leq \frac{1241}{Eg(eV)} \qquad \text{(eq. 1)}$$

Figure 1.

From UV-Vis-DR measurements, it can be concluded that pure minium becomes photoactive when exposed to light of wavelength below 605 nm (E_g = 2.05 eV). However the synthesized minium exhibits a slightly lower band gap energy (E_g = 1.98 eV). Since lower band gap energy initiates transition of electrons to the conduction band more easily, it becomes more reactive (photoactive). The mechanism for this higher photoactivity and the role of lead oxides is further discussed in the text. From the blue and red curves in Figure 1, the band gap of litharge and massicot can be determined to be 1.72 and 2.43 eV respectively.

3.2 Minium: a p-type semiconductor

A minium-coated graphite electrode was exposed to alternating cycles of darkness (~10 s) and illumination (~10 s) in an electrochemical set up; the resulting response in photocurrent is shown in Figure 2. The results show that minium is stable in the dark and exhibits a reduction photocurrent during blue laser illumination. Because it only becomes reactive during illumination, the photoactivity is only attributed to reaction of minority carriers, i.e. electrons. Hence minium is a p-type semiconductor.

During the illumination the photo-generated electrons are taken up by the minium and photodecomposition takes place where minium is primarily converted to PbO (equation 2), giving rise to a cathodic photocurrent.

$$Pb_3O_4 + 2H^+ + 2e^- \rightarrow [3PbO] + H_2O \qquad \text{(eq. 2)}$$

Figure 2.

Furthermore, the minium-coated graphite electrode was exposed to alternating cycles of darkness and red laser (650 nm, 30 mW) illumination. Since it has an energy below the absorbance band ($h\nu < E_g$) for minium, no photocurrent was generated.

Raman spectroscopy of the commercial minium powder was also used as a method to identify the photodegradation products of minium since it is known to be a strong Raman scatterer. Since minium absorbs light of a wavelength below 605 nm, the red laser excitation line (785 nm) was used to record Raman spectra without inducing undesired transformations. The Raman bands at 121, 390 and 550 cm^{-1} are known to be characteristic for (non-degraded) minium.[22] When exposed to green laser light (514 nm) at 100 % power (8.5 mW), a new laser induced degradation product is formed. The degradation product registered new bands at 86, 142 and 289 cm^{-1}, characteristic for massicot (β-PbO) (Figure 3). These observations suggest that upon absorption of light of sufficiently high energy, minium is primarily photodecomposed into PbO. A more elaborate study of this phenomenon revealed that the laser power determines whether massicot or litharge is formed; a higher laser power results in a higher proportion of massicot.[17]

3.3 Reactivity of minium in aqueous environment

To predict the reactivity of commercial minium in an aqueous environment, the energy positions of the valence and conduction bands are compared with the thermodynamic redox potential of the semiconductor. This method has recently been used as a screening technique for modelling the stability of semiconductor pigments in aqueous environment.[23] The thermodynamic oxidation (φ^{ox}) and reduction (φ^{red}) potential of minium (Figure 4) is determined from its Pourbaix diagram in a neutral pH aqueous environment at 25 ^{0}C.[24]

Figure 3.

Since the thermodynamic oxidation (φ^{ox}) and reduction (φ^{red}) potentials of minium are situated between those of water, it is unstable against both oxidation and reduction in water. This explains the different discolorations (redox changes) reported in minium degradation studies. However upon exposure to light in an aqueous environment, a cathodic photocurrent is exhibited indicating its predominant instability against reduction. The latter is consistent with the p-type semiconductor character of the material.

Figure 4.

3.4 Minium photoactivity in 0.01 M NaCl and $NaHCO_3/Na_2CO_3$ buffer solution

Upon exposure to various physical or chemical agents, semiconductors behave in different ways; a number of alteration products can be formed at different rates. In order to improve paint conservation strategies, it is therefore important to understand this manner of interaction. It is already well documented that dissolved atmospheric CO_2 plays a major role in the photodecomposition of minium[20] and that its degradation products quickly react in the presence of ionic carbonate/bicarbonate species. For this purpose, we studied the photoactivity of minium in two electrolytes: 0.01 M NaCl and $Na_2CO_3/NaHCO_3$ buffer solutions. A minium modified graphite electrode was exposed to blue laser light with alternating cycles of illumination and darkness (~10 s) in the two electrolytes (Figure 5). For a better understanding of the role of carbonates/bicarbonates in the buffer solution on the photoreactivity, a pH range of 8 to 11 was selected.

A significant difference in photocurrent magnitude is recorded between the two types of electrolyte solutions. In NaCl solution (pH = 7), a lower photocurrent is exhibited as compared to the $NaHCO_3/Na_2CO_3$ buffer solutions at pH 8 or 9. The lower photocurrent in

NaCl is likely to result from the sole reduction process of Pb_3O_4 to PbO. The higher photoreduction current that is recorded when a sodium bicarbonate/carbonate buffer is used as electrolyte is attributed to the subsequent reaction of PbO with bicarbonates, leading to the formation of hydrocerussite. The amount of hydrocerussite formed depends on the availability of bicarbonates, indicating their importance in the photodecomposition process of minium (Figure 5, B-E).

$$3PbO + 2HCO_3^- + H_2O \rightarrow Pb_3(CO_3)_2(OH)_2 + 2OH^- \quad \text{(eq. 3)}$$

Figure 5.

Furthermore, in the selected range of pH, a clear correlation between the photodecomposition of minium and the relative amount of bicarbonate in the buffer is discovered. The reduction photocurrent decreases exponentially with increasing pH. Since bicarbonates dominate at lower pH, it is clear that they play a significant role in the process of minium photodecomposition (inset Figure 5) and favor the degradation reactions.

To verify the formation of hydrocerussite as a degradation product in carbonate/bicarbonate buffer solution, minium-modified electrodes in contact with different solutions were intentionally degraded with an 8.5 mW green laser light (514.5 nm). Raman spectra before and after green laser degradation were taken on the same spot by means of a 785 nm Raman laser. The irradiated minium-covered electrodes were in contact with drops (20 µL) of NaCl and Na_2CO_3/$NaHCO_3$ buffer solutions. Fig. 6 shows the resulting Raman spectra after degradation (via green laser illumination). In the NaCl solution, the minium bands decrease in intensity while those of lead oxides increase (Figure 3). On the other hand, minium degraded in the buffer solution exhibits, next to lead carbonates (for example hydrocerussite at 411, 667, 681, 706 and 865 cm^{-1}), additional bands indicating the formation of (double) hydrated carbonate species.[25, 26] The formation of these hydrated carbonates, originating from the buffer solution, suppress some of the typical bands of the lead carbonates such as the band at 1054 cm^{-1} for cerussites. From 900 to 1150 cm^{-1} is the typical ν1 carbonate region, both lead carbonates and buffer carbonates such as $Na_2CO_3.NaHCO_3.2H_2O$ (trona) and $Na_2CO_3.H_2O$ are visible in this range. The ν4 bending mode of the carbonate of both cerussites and hydrated carbonates are observed at respectively 660-700 and 706-720 cm^{-1}.[27]

Figure 6.

3.5 The influence of the presence of lead (II) oxides on the photoactivity of minium

One of the photodegradation products of minium is lead (II) oxide which occurs in tetragonal and orthorhombic structural forms as litharge (α-PbO) and massicot (β-PbO) respectively. Since these degradation products also exhibit semiconductor behavior (Figure 1), it is vital to investigate their influence on the photoactivity of minium. It is well documented that minium used as artistic pigment contains variable amounts of litharge/massicot.[8, 11, 28] Since litharge has a lower band gap (1.73 eV) than massicot (2.43 eV), it is expected to be more photoactive. The effect of PbO nanoclusters was previously described in relation to the photoactivity of rutile.[29]

To evaluate the influence of the presence of PbO on the photoactivity of minium, we compared the photocurrent response generated from commercial minium and synthesized minium when in contact with $NaHCO_3$/Na_2CO_3 buffer solution at pH 8. Figure 7 shows that the synthesized minium (with ca 5% PbO) is found to be a factor 1.7 more photoactive than commercial minium (i.e.,

PbO-free) (Figure 7). We attribute this higher reactivity to the introduction of new states in the original band gap of minium due to newly formed Pb-O interfacial bonds. The PbO nanocluster modification brings about an upwards shift of the valence band, which reduces the band gap (from 2.05 to 1.98 eV – see Figure 5) and result in higher photoactivity. Therefore in realistic situations (minium used in paintings originally synthesized by calcination of litharge), minium photodegradation is exacerbated by the presence of unreacted litharge in it. It should be noted that comparison of the photocurrent with pure litharge (α-PbO) was not possible because (self-synthesized) α-PbO nanoparticles do not adsorb completely on the graphite surface. After deposition and during contact with the electrolyte, the material is easily detached from the surface and electrochemical detection is no longer reproducible.

Figure 7.

3.6 Degradation kinetics of commercial and synthesized minium

Understanding pigment degradation processes and the prediction of (environmental) harmful conditions is highly significant in the preservation of historical paintings. Electrochemical methods of detection provide vital information on how fast pigment degradation occur under variable environmental conditions. For this purpose a graphite|pigment electrode is positioned in an electrochemical cell and irradiated with a blue laser (405 nm). By employing amperometry, details on the degradation process are gathered in a fast way by providing information on the changes in photocurrent intensity.

To study the degradation kinetics, the experiments in the electrochemical cell were carried out by exposing the pigment modified electrode to an alternating cycles of darkness (~ 10 s) and illumination (~ 10 s) at a constant potential. Electrochemical experiments were performed in a pH 8 of 0.01 M $NaHCO_3/Na_2CO_3$ buffer solution after modifying the surface of the electrode with commercial and synthesized minium and the recorded photocurrent was used to characterize the pigment layer. Electrodes with freshly deposited pigments showed noticeable well-detectable photocurrents while a bare graphite electrode showed no photocurrent. Since the photocurrent is dependent on the amount of pigment on the electrode, a gradual decrease in photocurrent is expected when commercial (synthesized) minium becomes more degraded. A decrease in photocurrent intensity was recorded after every 60 seconds of illumination. Figure 8 indicates that after 540 seconds of illumination, a higher percentage of synthesized minium (ca 70 %) is already degraded compared to ca 55% of the commercial minium. Accordingly, the synthetized minium reaches its degradation half-time (~120 seconds) more quickly than the commercial minium (~300 seconds). The order of the reaction was also determined by plotting the natural logarithm of the photocurrent as a function of time. The curve follows a linear trend with negative slope for both commercial ($k=0.0065\ s^{-1}$) and synthesized ($k=0.0079\ s^{-1}$) minium indicating a first order reaction. Based on the values of the slope (rate constants), the degradation kinetics experiment also revealed that synthesized minium is more photoactive (22% times) than the commercial one due to the 5% litharge content in it.

Figure 8.

4. CONCLUSION

By means of electrochemical experiments we were able to show that the semiconductor pigment minium becomes photoactive upon exposure to light with photon energy larger than its band gap (2.1 eV; 590 nm). Since the pigment is unstable towards both

oxidation and reduction against water, it may give rise to different discoloration phenomena and corresponding degradation products. The photoreduction current registered during exposure to visible light and its lack of reactivity in darkness suggests that minium is a p-type semiconductor. Upon exposure to light, the promotion of electrons from the valence band to the conduction band initializes the reduction Pb(IV) to Pb(II), leading to an initial formation of PbO. Minium that originally contains (residual) litharge features a slightly different band gap due to the introduction of new electronic states through PbO/Pb_3O_4 interfacial bonds. The new states shift the valence band upward, inducing more efficient electron/hole separation and hence higher conductivity. Furthermore, the significantly higher photocurrent intensity recorded in $NaHCO_3/Na_2CO_3$ buffer compared to a NaCl solution is attributed to the subsequent reaction of PbO with bicarbonates to form (hydro)cerussite. In the presence of bicarbonate ions, the photoreactivity of minium is highly enhanced.

In summary it can be stated that next to the wavelength of the light and the concentration of (bi)carbonate ions in the environment, the photodegradation of minium is also dependent on the purity of the pigment. The presence of impurities that decrease the band gap energy of the semiconductor pigment facilitate the rate of degradation.

AUTHOR INFORMATION

Corresponding Author

* Email: Karolien.DeWael@uantwerpen.be

Notes

The authors declare no competing financial interest.

ACKNOWLEDGMENTS

The authors acknowledge Sanne Aerts from the Laboratory of Adsorption and Catalysis (LADCA) of the University of Antwerp for her help with the UV-Vis-DR.

REFERENCES

1. A. Roy and R. L. Feller, *Artists' pigments: a handbook of their history and characteristics*, National Gallery of Art, Washington, 1986.
2. S. Daniilia, E. Minopoulou, K. S. Andrikopoulos, A. Tsakalof and K. Bairachtari, *Journal of Archaeological Science*, 2008, **35**, 2474-2485.
3. H. G. M. Edwards, D. W. Farwell, E. M. Newton, F. Rull Perez and S. Jorge Villar, *Journal of Raman Spectroscopy*, 2000, **31**, 407-413.
4. J. P. McKinley, M. K. Dlaska and R. Batson, *Journal of Power Sources*, 2002, **107**, 180-186.
5. J. Wang, S. Zhong, H. K. Liu and S. X. Dou, *Journal of Power Sources*, 2003, **113**, 371-375.
6. D. P. Boden, *Journal of Power Sources*, 1998, **73**, 56-59.
7. H. J. Terpstra, R. A. De Groot and C. Haas, *Journal of Physics and Chemistry of Solids*, 1997, **58**, 561-566.
8. D. Saunders, M. Spring and C. Higgitt, 2002.
9. E. Kotulanová, P. Bezdička, D. Hradil, J. Hradilová, S. Švarcová and T. Grygar, *Journal of Cultural Heritage*, 2009, **10**, 367-378.
10. S. Aze, J.-M. Vallet, M. Pompey, A. Baronnet and O. Grauby, *Eur. J. Mineral*, 2007, **19**, 883-890.
11. S. Aze, J. M. Vallet, V. Detalle, O. Grauby and A. Baronnet, *Phase Transitions*, 2008, **81**, 145-154.
12. D. Sister and E. Minopoulou, *Applied Physics a-Materials Science & Processing*, 2009, **96**, 701-711.
13. H. Catherine, S. Marika and S. David, *Journal*, 2003, **24**, 75-95.
14. P. A. Christensen, A. Dilks, T. A. Egerton, E. J. Lawson and J. Temperley, *Journal of Materials Science*, 2002, **37**, 4901-4909.
15. F. Vanmeert, G. Van der Snickt and K. Janssens, *Angewandte Chemie International Edition*, 2015, **54**, 3607-3610.
16. Y. G. Zhou, J. L. Long, Q. Gu, H. X. Lin, H. Lin and X. X. Wang, *Inorganic Chemistry*, 2012, **51**, 12594-12596.

17. L. Burgio, R. J. H. Clark and S. Firth, *Analyst*, 2001, **126**, 222-227.
18. P. Baraldi, C. Fagnano and P. Bensi, *Journal of Raman Spectroscopy*, 2006, **37**, 1104-1110.
19. W. Anaf, S. Trashin, O. Schalm, D. van Dorp, K. Janssens and K. De Wael, *Analytical Chemistry*, 2014, **86**, 9742-9748.
20. Y. Zhou, H. Lin, Q. Gu, J. Long and X. Wang, *RSC Advances*, 2012, **2**, 12624-12627.
21. D. L. Perry and T. J. Wilkinson, *Appl. Phys. A*, 2007, **89**, 77-80.
22. H. G. M. Edwards, D. W. Farwell, E. M. Newton and F. Rull Perez, *Analyst*, 1999, **124**, 1323-1326.
23. W. Anaf, O. Schalm, K. Janssens and K. De Wael, *Dyes and Pigments*, 2015, **113**, 409-415.
24. K. Dong-Su and W. Yu-Ra, *Journal of Korea Society of Waste Management*, 2013, **30**, 60-67.
25. M. H. Brooker, S. Sunder, P. Taylor and V. J. Lopata, *Canadian Journal of Chemistry*, 1983, **61**, 494-502.
26. M.-C. Bernard, V. Costa and S. Joiret, *e-Preservation science*, 2009, **6**, 101-106.
27. W. N. Martens, L. Rintoul, J. T. Kloprogge and R.L. Frost, *American Mineralogist*, 2004, **89**, 352-358.
28. G. Trefalt, B. Malič, D. Kuščer, J. Holc and M. Kosec, *Journal of the American Ceramic Society*, 2011, **94**, 2846-2856.
29. A. Iwaszuk and M. Nolan, *Catalysis Science & Technology*, 2013, **3**, 2000-2008.

FIGURE CAPTIONS

Figure 1. UV-Vis-DR (UV-Visible Diffuse Reflectance) spectrum of commercial minium, synthesized minium, litharge and massicot.

Figure 2. Minium photoactivity during darkness and illumination in a 0.01 M NaCl solution using a) a red laser (650 nm) and (b) a blue laser (405 nm) for illumination.

Figure 3. Raman spectra taken with the red laser for commercial minium (red curve) and its green laser induced degradation product (green curve).

Figure 4. Oxidation and reduction potentials of minium with respect to the redox potential of water.

Figure 5. Minium photoactivity in 0.01 M NaCl (A) and $NaHCO_3/Na_2CO_3$ (B-E) buffer solution under blue laser illumination [pH 11 (B), pH 10 (C), pH 9 (D) and pH 8 (E)].

Figure 6. Raman spectra of green laser degraded minium in 0.01 M $NaHCO_3/Na_2CO_3$

Figure 7. Photocurrent comparison between pure minium (a) and synthesized minium (b) in a pH 8 0.01 M $NaHCO_3/Na_2CO_3$ buffer solution under blue laser illumination.

Figure 8. Degradation kinetics of commercial minium (dots) and synthesized minium containing litharge (squares) in a pH 8 0.01 M $NaHCO_3/Na_2CO_3$ buffer solution under blue laser light illumination (405 nm).

FIGURES

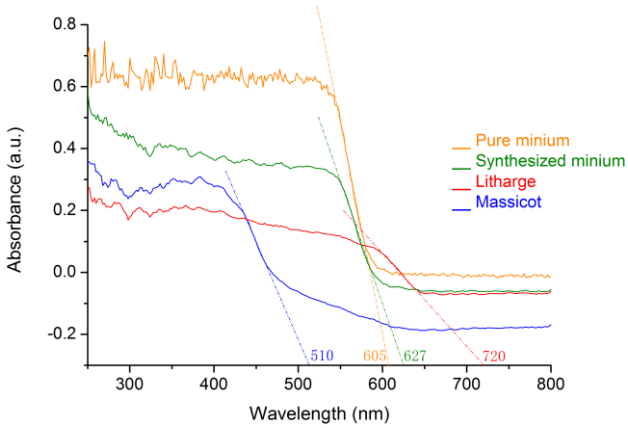

Figure 1

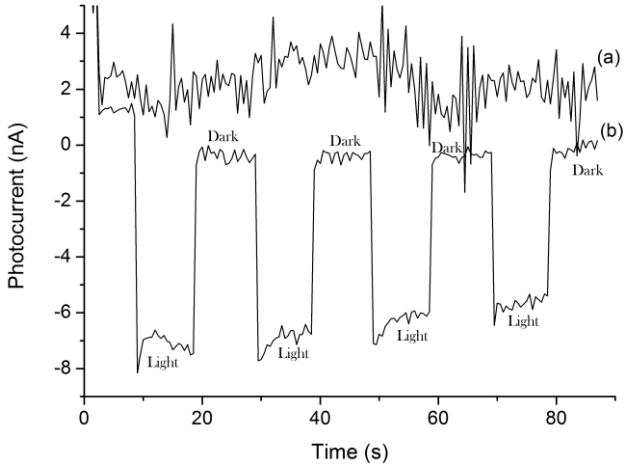

Figure 2

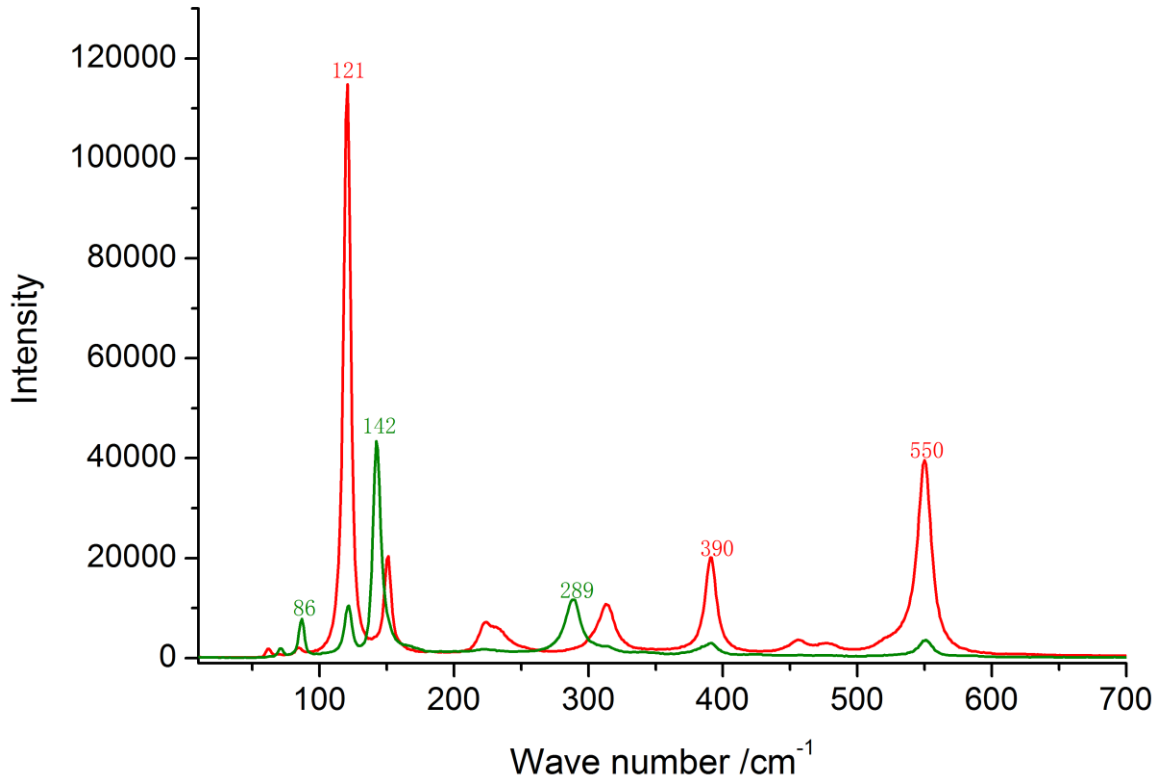
120000
100000
80000
60000
40000
20000
0
Intensity
121
142
86
289
390
550
100
200
300
400
500
600
700
Wave number /cm-1

Figure 3

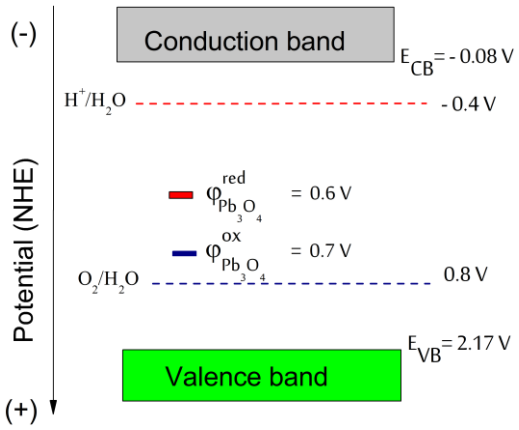
(-)
Conduction band
E_{CB} = - 0.08 V
H^+/H_2O
- 0.4 V
Potential (NHE)
$\varphi^{red}_{Pb_3O_4}$ = 0.6 V
$\varphi^{ox}_{Pb_3O_4}$ = 0.7 V
O_2/H_2O
0.8 V
E_{VB} = 2.17 V
Valence band
(+)

Figure 4

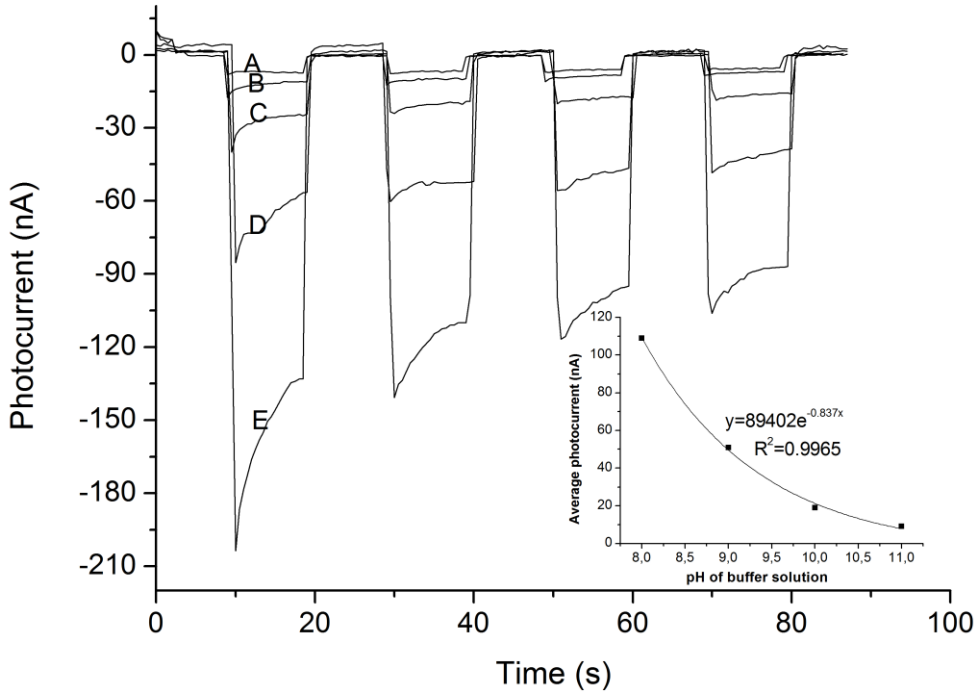
Photocurrent (nA)
Time (s)
A
B
C
D
E
Average photocurrent (nA)
pH of buffer solution
y=89402e-0.837x
R2=0.9965

Figure 5

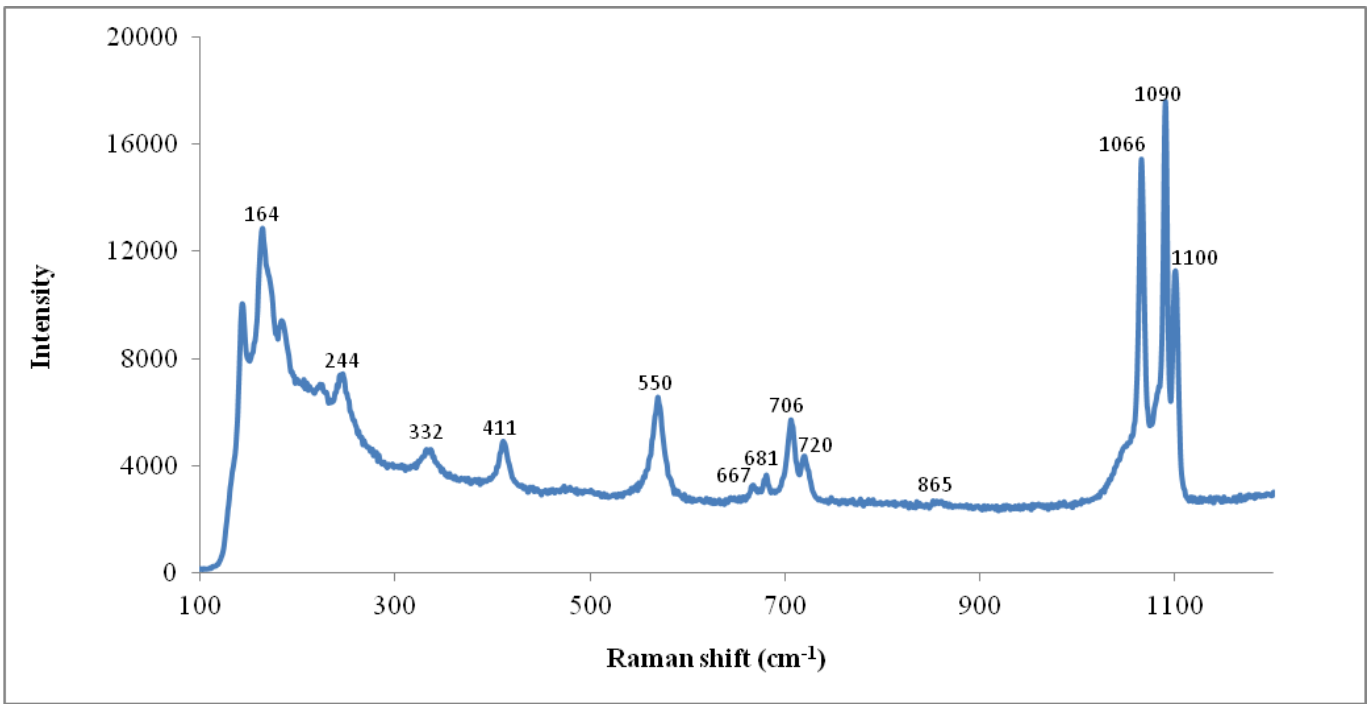
20000
16000
12000
8000
4000
0
Intensity
100
300
500
700
900
1100
Raman shift (cm-1)
164
244
332
411
550
667
681
706
720
865
1066
1090
1100

Figure 6

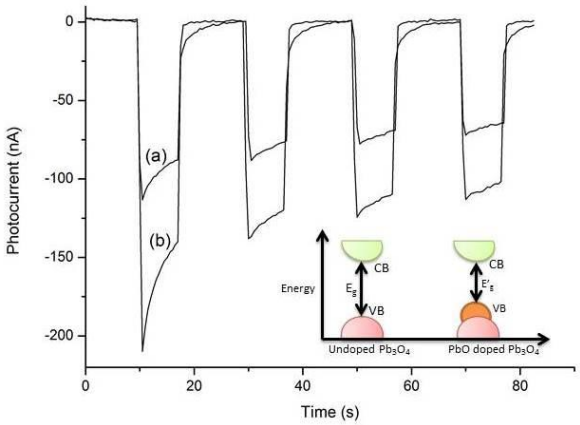
Photocurrent (nA)
0
-50
-100
-150
-200
(a)
(b)
0
20
40
60
80
Time (s)
Energy
CB
VB
E_g
CB
VB
E'_g
Undoped Pb_3O_4
PbO doped Pb_3O_4

Figure 7

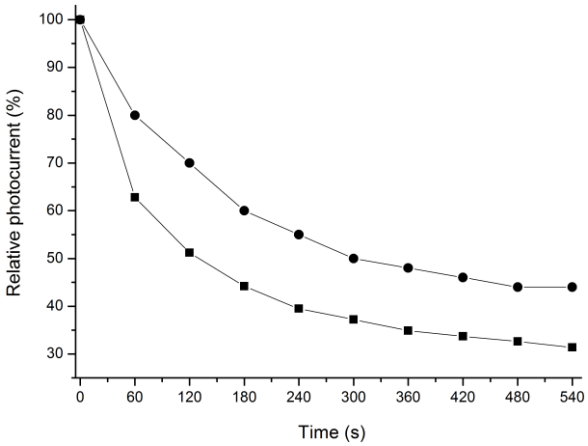
Relative photocurrent (%)
100
90
80
70
60
50
40
30
0
60
120
180
240
300
360
420
480
540
Time (s)

Figure 8